Food and Chemical Toxicology 126 (2019) 211–222

Contents lists available at ScienceDirect

Food and Chemical Toxicology

journal homepage: www.elsevier.com/locate/foodchemtox

Camellia euphlebia protects against corticosterone-induced apoptosis in differentiated PC12 cells by regulating the mitochondrial apoptotic pathway and PKA/CREB/BDNF signaling pathway

Dongye He[a], Ning Wang[b,c], Xuan Sai[b,c], Xiaoyu Li[b,c], Yongping Xu[b,c,*]

[a] Department of Central Laboratory, Affiliated Hospital of Jining Medical University, Jining Medical University, Jining, 272000, China
[b] School of Life Science and Biotechnology, Dalian University of Technology, Dalian, 116024, China
[c] Ministry of Education Center for Food Safety of Animal Origin, Dalian University of Technology, Dalian, 116620, China

ARTICLE INFO

Keywords:
Camellia euphlebia
Corticosterone
Neurotoxicity
Differentiated PC12 cells
Apoptosis
Brain derived neurotrophic factor

ABSTRACT

Camellia euphlebia is a Chinese folk medicine, known for its multiple pharmacological properties. Our previous studies have demonstrated its antidepressant activity by several animal models of depression. The possible underlying mechanism was further explored by investigating the neuroprotective effect of *Camellia euphlebia* extract (CEE) on corticosterone-induced apoptosis in neuronally differentiated PC12 cells. The results of methylthiazolyl-tetrazolium assay, lactate dehydrogenase release assay, Hoechst 33342 staining, propidium iodide staining, AV-FITC/PI double staining and DNA fragmentation analysis consistently indicated that pretreatment of PC12 cells with CEE at 20–80 μg/mL significantly reversed 300 μmol/L corticosterone-induced apoptosis in a dose dependent manner. Furthermore, intracellular mitochondrial membrane potential, reactive oxygen species accumulation, calcium level, Bcl-2/Bax ratio, caspase activity were assessed, and the results indicated that CEE exhibited its anti-apoptotic effect through the regulation of mitochondrial apoptosis pathway. Additionally, CEE increased the cyclic adenosine monophosphate-dependent protein kinase (PKA) level, which phosphorylated cAMP response element binding protein (CREB), and finally elevated the mRNA expression of brain-derived neurotrophic factor (BDNF) gene. It is speculated that the antidepressant effect of CEE *in vivo* may be associated with the cytoprotection of neuron damaged by corticosterone, and the cellular mechanism involves the mitochondrial-mediated apoptosis and PKA-CREB-BDNF signaling pathway.

1. Introduction

Depression is a very common psychotic mood disorders characterized by some of the core symptoms including depressed mood, slowed thinking, anhedonia, severe fear and cognitive impairment (Vos et al., 2016). The incidence and mortality of depression are very high, and it has been recognized as a serious threat for human health, as well as creates a huge economic burden in the worldwide. The World Health Organization estimated that depression affects more than 300 million people and 76.4 millions are lost to disability each year owing to depression worldwide (WHO, 2017; Smith, 2014). Although concerns about depression have been expressed for a long time, the exact pathogenic mechanisms are still unclear. In recent years, a substantial amount of experimental and clinical data has supported the notion that hyperactivity of the hypothalamic-pituitary-adrenal (HPA) axis is involved in the pathogenesis (Cowen, 2010; Keller et al., 2017). It is well known that the HPA axis is activated in response to stress, which results in the increased concentrations of glucocorticoids in the circulating blood (Micale and Drago, 2018). High levels of corticosterone, a principal glucocorticoid, have been found to cause pathological damage to the hippocampal neurons both *in vitro* and *in vivo*, and can induce depression-like behavior in animals which could be reversed by antidepressants (Pariante and Lightman, 2008). Furthermore, the reduced hippocampal volumes and decreased hippocampal cells were observed in depression patients by magnetic resonance imaging study and postmortem analyses (Huang et al., 2013). Therefore, it is speculated that the protection against neuron damage induced by high concentration of corticosterone might be a potential mechanisms of antidepressant agents.

Camellia euphlebia Merr. Ex Sealy (Theaceae), an evergreen shrub with a natural distribution limited to North Vietnam and Southwest China, appeared in Chinese medical classics Ben Cao Gang Mu about

* Corresponding author. School of Life Science and Biotechnology, Dalian University of Technology, Dalian, 116024, China.
E-mail addresses: 912799291@qq.com (D. He), 707986264@qq.com (N. Wang), 714942452@qq.com (X. Sai), 6888544@qq.com (X. Li), hehe0917@mail.jnmc.edu.cn (Y. Xu).

https://doi.org/10.1016/j.fct.2019.02.028
Received 19 September 2018; Received in revised form 11 February 2019; Accepted 18 February 2019
Available online 25 February 2019
0278-6915/

400 years ago and has been widely used to treat tumor, nephritis, hepatitis with jaundice, urinary tract infection, dysentery, hypertention, diarrhea, faucitis and irregular menstruation (He et al., 2018a,b). Our previous work also demonstrated that *Camellia euphlebia* extract (CEE, thereafter) possessed antidepressant-like effect in several animal behavioral tests including forced swimming test, tail suspension test and chronic unpredictable mild stress test, and the antidepressant-like effect of CEE appeared to involve the alteration of hypothalamic-pituitary-adrenal axis and monoaminergic systems *in vivo* (He et al., 2015, 2018a). However, the cellular and molecular mechanisms in the antidepressant-like effect of CEE is still not clear. As a lot of studies have proved that the atrophy and loss of neurons in hippocampus, prefrontal cortex, lateral habenular nucleus or amygdaloid nucleus regions play a key role in the pathogenesis of depression (Miller and Hen, 2015). Therefore, there is a reason to believe that neuroprotective effect might be contributing to the *in vivo* antidepressant-like effect.

The differentiated rat pheochromocytoma (PC12) cell line induced by nerve growth factor (NGF), possesses typical neuron features and expresses a high level of glucocorticoid receptors, making them sensitive to glucocorticoids exposure (Zou et al., 2016). Currently, differentiated PC12 cells has been widely used as a *in vitro* modeling in neurobiological or neuromolecular mechanisms underlying the antidepressant effect of drugs (Jiang et al., 2015). Therefore, the present study aimed to investigate the protective effects of CEE on the corticosterone-induced neurotoxicity and its possible mechanisms in differentiated PC12 cells.

2. Materials and methods

2.1. Reagents

Rutin, caffeine, L-theanine, quercetin and ginsenoside Rg1 were purchased from Chengdu Must Biotechnology (Chengdu, China). Dulbecco's Modified Eagle Medium (DMEM) and fetal bovine serum (FBS) were purchased from Gibco (Grand Island, NY, USA). Horse serum (HS) was obtained from Invitrogen (Carlsbad, CA, USA). Methyl thiazolyl tetrazolium (MTT), Hoechst 33342, propidium iodide (PI), bovine serum albium (BSA), mitochondrial membrane potential (MMP) assay kit and super signal West Pico ECL substrate were purchased from Solarbio Life Sciences (Beijing, China). Penicillin, streptomycin, DNA ladder extraction kit, 2′, 7′-dichlorfluorescein diacetate (DCFH-DA), Fura-2/AM and Caspase-3/9 assay kit were supplied from Beyotime Biotechnology (Shanghai, China). Corticosterone (purity ≥ 98.5%) and nerve growth factor (NGF, purity ≥ 97%) were purchased from Sigma-Aldrich (St Louis, MO, USA). Lactate dehydrogenase (LDH) assay kit and BCA protein assay kit were obtained from Nanjing Jiancheng Bioengineering Institute (Nanjing, China). PKA ELISA kit purchased from Lengton Biotechnology (Shanghai, China). Annexin V-fluorescein isothiocyanate/propidium iodide (AV-FITC/PI) was purchased from Beijing You Yi Zhong Lian Biotechnology (Beijing, China). MiniBEST universal RNA extraction kit, PrimeScript RT reagent kit and SYBR Premix Ex Taq II were purchased from TaKaRa (Otsu, Shiga, Japan). Anti-Bcl-2 and anti-Bax antibodies were purchased from Wanlei Biotechnology (Shenyang, China). Anti-*p*-CREB antibody was obtained from Santa Cruz Biotechnology (Santa Cruz, CA, USA). All secondary antibodies were supplied by Abbkine (Redlands, CA, USA). All other chemicals and reagents were of analytical grade.

2.2. Plant material and preparation of extract

Fresh leaves of *Camellia euphlebia* Merr. ex Sealy were obtained from Guangxi Zhuang Autonomous Region during its flowering period. The specimen was authenticated by Dr. Zhonghhui Ma (Department of Botany Sciences, College of Agriculture, Guangxi University, China). A voucher specimen with number 8109255 has been deposited in the herbarium of Guangxi Institute of Botany, Chinese Academy of Sciences, China.

Preparation of *Camellia euphlebia* extract was performed as described in our previous work (He et al., 2018a). Briefly, the leaves were ground into a ultrafine powder with an energy-intensive vibrational mill. Twenty grams of the fine power was suspended in 300 mL distilled water and subjected to ultrasound-assisted extraction for 30 min at 70 °C at frequency of 40 KHz using an open rectangular ultrasonic processor. After that, the mixture was centrifuged at 10000 × *g* for 10 min and the supernatant was filtered through a 0.22-μm Millipore Filter to remove the particulate matter. The filtrate was freeze dried using a freeze dryer. The extract was stored in a sealed bag at −20 °C until use.

2.3. Phytochemical analysis

2.3.1. HPLC-MS analysis

HPLC-MS analyses were operated using an Agilent 1100 liquid chromatography system, equipped with Agilent 6130 MS system. An Agilent HPLC Ultimate polar-Rp (2.1 × 150 mm, 5 μm) was used with an injection volume of 2 μL for the HPLC separation. The binary mobile phase was water-ammonium chloride (99.5: 0.5, v/v) (A) and methanol (B) with the following gradient elution programme: 5% B (0–35 min), 60% B (35–45 min), 100% B (45–55 min). The peaks were detected at 220 nm, and the flow rate was set at 0.4 mL/min at room temperature. The positive ion mode was used for further characterization of the compounds. The heated capillary and spray voltage were maintained at 350 °C and 3.0 kV, respectively. Nitrogen was at 40 psi for sheath gas flow rate and full scan mass spectra from m/z 80–1000 were recorded with a scan speed of one scan per second. Quercetin, rutin, caffeine, L-theanine and ginsenoside Rg1 were identified by comparison of their molecular ions (m/z) and retention times with authentic standard (Fig. 1).

2.3.2. HPLC analysis

L-theanine and ginsenoside Rg1 without conjugated double bonds, both have low absorption in the ultraviolet region, therefore, the present study only measured the contents of quercetin, rutin and caffeine by HPLC. HPLC analyses were performed on a Agilent HPLC system equipped with a PDA detector scanning from 210 to 400 nm, a XB-C_{18} column at a column temperature of 25 °C, and an autosampler. The binary mobile phase was water-acetic acid (99.5: 0.5, v/v) (A) and methanol (B) with the following gradient elution programme: 30% B (0–20 min), 70% B (20–30 min), 100% B (30–40 min). The injection volume of each sample was 5 μL and the flow rate of the mobile phase was set at 0.8 mL/min. Quercetin, rutin and caffeine were further confirmed based on retention time, and the concentrations of three compounds were calculated by comparing their peak area with those of corresponding standards (Figs. 1S and 2S, supplementary material). The content of quercetin, rutin and caffeine were 4.60 ± 0.87 mg/g, 3.23 ± 0.83 mg/g, 11.51 ± 0.99 mg/g.

2.4. Cell culture and treatment

Rat pheochromocytoma PC12 cells were obtained from Cell Bank of Shanghai Institute of life Science (SCSP-517, Chinese Academy of Sciences, Shanghai, China) and were cultured in DMEM medium supplemented with 10% heat-inactivated FBS, 5% heat-inactivated HS, 100 U/mL penicillin and 100 μg/mL streptomycin at 37 °C in a humidified atmosphere of 5% CO_2 and 95% air. For differentiation, PC12 cells were grown on 25 cm^2 plastic flask and kept in serum-containing medium for three to four days. Subsequently, to facilitate neurite outgrowth, cells were differentiated in 10% FBS medium supplemented with NGF (20 ng/mL) for seven to ten days. Fresh NGF was added every second day with the medium change. Differentiated PC12 cells were cultured in DMEM medium only supplemented with 10% heat-inactivated FBS and used for further experiments. For cell growth curve, differentiated

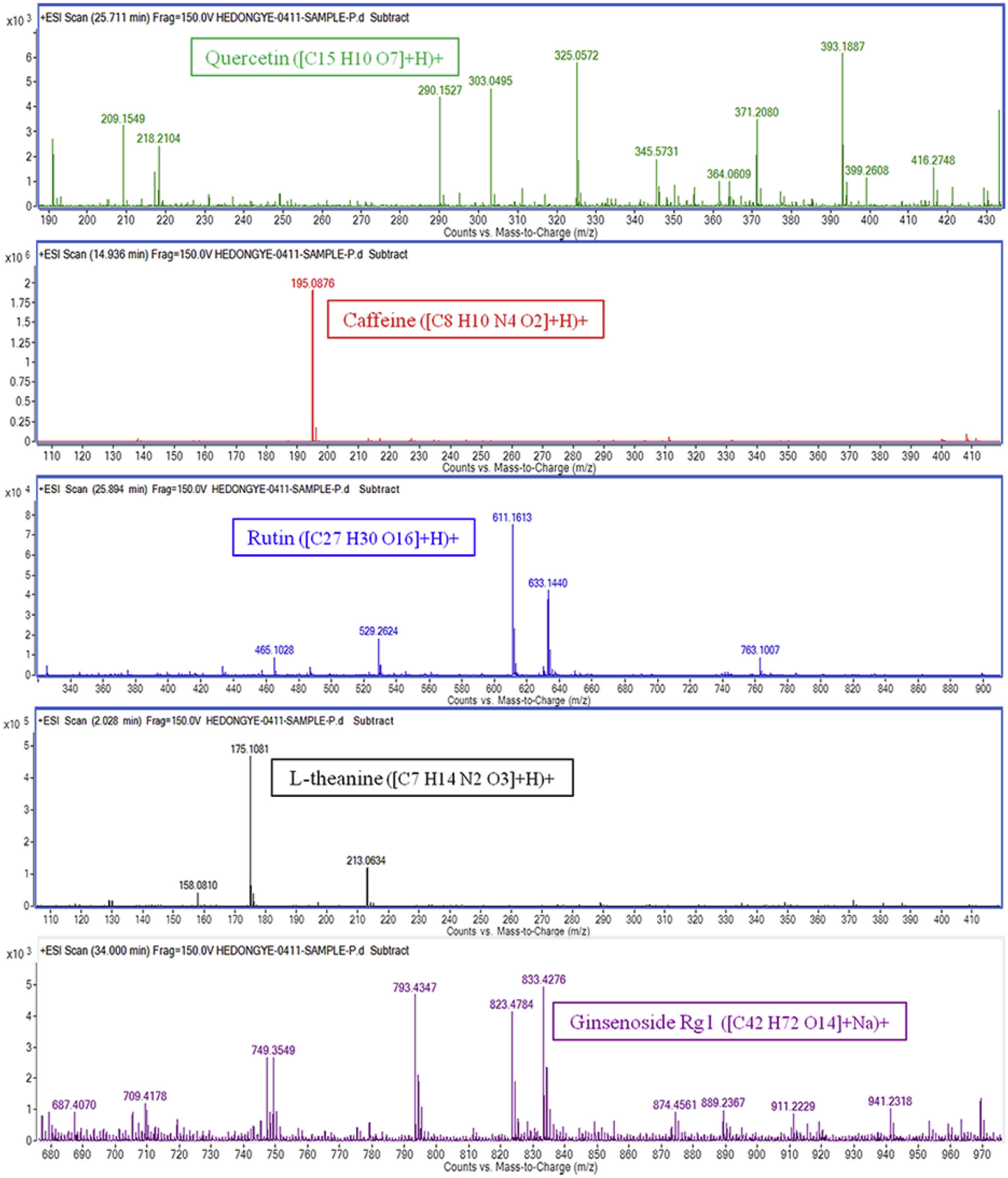

Fig. 1. Representative total ion chromatogram of HPLC/MS analysis of *Camellia euphlebia* extract (CEE).

PC12 cells were seeded in 6-well plates (2×10^4 cells per well) in triplicate and divided into seven groups. The number of differentiated PC12 cells per group was counted every day for 7 day to generate a growth curve (Fig. 3S, supplementary material). The doubling time of differentiated PC12 cells calculated by the formula: TD = t × [lg2/(lgNt-lgN_0)] (Huang et al., 2012), was approximately 32 h. Differentiated PC12 cells in logarithmic growth phase would be used for subsequent experiments.

The appropriate damage concentration of corticosterone was selected on the basis of our previous work (Fig. 4S, supplementary material). In brief, when treated with 300 μM corticosterone for 24 h, the differentiated PC12 cells viability decreased to 56.70%, and was used in

subsequent experiments. To research the neuroprotective effect of CEE, the cells were divided into three equal groups: non-treated control, 300 μM corticosterone and 300 μM corticosterone plus CEE (10, 20, 40, 80, 160 and 320 μg/mL) or each identified components (L-theanine, caffeine, quercetin, rutin, ginsenoside Rg1) in the experiments. Experiments were executed for 24 h after the cells were seeded. CEE were applied for 24 h prior to the treatment with corticosterone, and then the cells were co-incubated with corticosterone and CEE for another 24 h.

2.5. Cell viability assay

Cell viability was determined by using the MTT assay, which is based on the conversion of MTT to formazan crystals by mitochondrial dehydrogenases (Morabito et al., 2010). At the end of the treatment, the medium was carefully removed and fresh medium containing 0.5 mg/mL MTT was then added to the cells followed by 4-h incubation at 37 °C. After that, the culture medium was replaced with an equal volume of dimethyl sulphoxide (DMSO) followed by 10-min incubation at room temperature. The absorbance of the plate was then measured at 570 nm by using a Multiskan GO microplate spectrophotometer (Thermo Fisher Scientific, Vantaa, Finland). Cell viability was expressed as percentage of control (non-treated) cells.

2.6. Lactate dehydrogenase (LDH) release assay

Cytotoxicity was quantitatively assessed by measuring the activity of lactate dehydrogenase (LDH) in the culture medium (He et al., 2018a,b). At the end of the treatment, the plate was centrifuged at 4000 × *g*/4 °C for 5 min to collect the supernatant fraction. The cell pellet was lysed with cell lysis buffer containing 1% Trition X-100. LDH activity in the supernatant and cell lysate was measured with an LDH assay kit according to the manufacturer's protocol. The rate of LDH release was calculated using the formula: (Supernatant value − blank value)/[(Supernatant value blank value) + (lysates value − blank value)] 100%.

2.7. Hoechst 33342 and PI staining assay

Hoechst 33342 staining distinguishing apoptotic from normal cells based on nuclear chromatin condensation and fragmentation was used for the qualitative analyses of the apoptotic cells. Likewise, PI can stain the nuclear changes of living and apoptotic cells. Differentiated PC12 cells were cultured in 6-well plates (5×10^4 cells per well) for 24 h. After treatment, the cells were incubated 1 mL Hoechst 33342 or 100 μL of 6.7 μg/mL PI for 20–30 min, washed twice with PBS, and then visualized by inverted fluorescence microscopy (IX71 + DP71, Olympus, Japan).

2.8. DNA fragmentation analysis

Differentiated PC12 cells were seeded at a density of 1×10^6 cells/well in 6-well microplates for 24 h. At the end of the treatment, the plate was centrifuged at 2000 × *g*/4 °C for 2 min to collect the cells. Subsequently, DNA was extracted by DNA ladder extraction kit according to the manufacture's instructions (C007, Beyotime Biotechnology). Fragmented DNA was analyzed electrophoretically on 1% agarose gel containing ethidium bromide. DNA Molecular Weight Marker (TaKaRa) was loaded in parallel in each experiment.

2.9. AV-FITC/PI double staining assay

Apoptosis was quantified by staining cells with AV-FITC and PI labeling (Wu et al., 2013). Briefly, differentiated PC12 cells were seeded at density of 1×10^6 cells/well in 6-well microplates for 24 h. After incubation, cells were co-incubated with 300 μM of corticosterone and different concentrations of CEE (20, 40, 80 and 160 μg/mL) for another 24 h. At the end of treatment, harvested cells were washed three times with cold PBS and resuspended in 100 μL cold PBS. Then 5 μL of AV-FITC and 10 μL of PI were added to cells and incubated at room temperature in the dark for 15 min and 400 μL PBS was added to each sample. The flow cytometric analysis was performed within 1 h.

2.10. Measurement of mitochondrial membrane potential (MMP)

5, 5′, 6, 6′-Tetrachloro-1, 1′, 3, 3′-tetraethylbenzimidazolyl-carbocya-nineiodide (JC-1) was used to determine the changes on MMP in corticosterone-treated differentiated PC12 cells. In brief, the cells were cultured in complete medium at a density of 1×10^6 cells/mL in 6-well plates, and then incubated with 2 mL JC-1 staining solution for 20 min in the darkness. After incubation, the cells were washed twice with JC-1 staining buffer and visualized by using an inverted fluorescence microscopy (IX71 + DP71, Olympus, Japan). Monomeric JC-1 green fluorescence emission and aggregate JC-1 red fluorescence emission were measured on a microplate reader (Varioskan Flash, Thermo Fisher, MA, USA). The exciting wavelength of monomeric JC-1 and aggregate JC-1 were set at 490 nm and 525 nm, respectively. The MMP of cells in all treatment groups was calculated as the ratio of red to green fluorescence.

2.11. Measurement of bcl-2/bax expression ratio

The level of bcl-2 and bax expression were measured by a flow-cytometric immunofluorescent method. Differentiated PC12 cells were seeded at density of 1×10^6 cells/well in 6-well microplates for 24 h. After treatment, the cells were collected by centrifugation at 1000 × *g* for 5 min and washed twice with PBS. Subsequently, the cells were fixed in 2% paraformaldehyde in PBS for 20 min at room temperature and lysed in 0.5% Triton X-100 for 30 min. The cells were then incubated with the specific primary anti-bcl-2 or anti-bax antibody (1: 150) at 4 °C overnight. FITC-conjugated goat anti-rabbit IgG was used as secondary antibody (1: 150) and incubated with cells at 37 °C in the dark for 1 h. Following twice washes with PBS. Fluorescence intensity was analyzed by flow cytometry (FACSCanto, BD Biosciences, San Diego, CA).

2.12. Measurement of intracellular ROS

ROS level was measured by using DCFH-DA method (Zhao et al., 2018). DCFH-DA is a non-fluorescent compound, and it can be enzymatically converted to highly fluorescent compound, DCF, in the presence of ROS. In brief, after the treatment, differentiated PC12 cells were incubated with DCFH-DA at a final concentration of 10 μM for 30 min at 37 °C in darkness. The fluorescence intensity was measured in the microplate reader (Varioskan Flash, Thermo Fisher, MA, USA) at an excitation wavelength of 488 nm and an emission wavelength of 525 nm after the cells were washed three times with serum-free medium to remove the extracellular DCFH-DA. The level of intracellular ROS was showed as a percentage of non-treated control.

2.13. Measurement of intracellular calcium level

The concentration of $[Ca^{2+}]_i$ was determined as described previously elsewhere (Anderson et al., 2015). In brief, Differentiated PC12 cells were plated on 24-well plates at a density of 1×10^5 cells/mL. At the end of the treatment, the cells were collected and incubated with cultured medium containing 5 μM Fura-2/AM at 37 °C for 45 min. Subsequently, the cells were washed with PBS and incubated with cold balanced salt solution buffer containing 0.2% bovine serum albumin at 37 °C for 5 min. The ratio of fluorescence intensities was determined by alternating excitation wavelengths of between 340 and 380 nm with emission at 510 nm, using a fluorescence spectrophotometer (F-4500, Hitachi, Japan). The concentration of $[Ca^{2+}]_i$ was calculated using the formula: $[Ca^{2+}]_i = K_d\ (F_0/Fs)\ (R\text{-}R_{min})/(R_{max}\text{-}R)$; $R = F_{340nm}/F_{380nm}$.

2.14. Caspase 3 and caspase 9 activity assays

Cellular caspase-3 and caspase-9 activities were measured with commercially available colorimetric assay kit (Beyotime Biotechnology, Shanghai, China). Differentiated PC12 cells were lysed with lysis buffer supplied with the kit. Then the soluble fraction of the cell lysate was assayed for caspase-3 and caspase-9 activities according to the manufacturer's protocol (Ac-DEVD-pNA as colorimetric substrate for caspase-3, and Ac-LEHD-pNA as colorimetric substrate for caspase-9). The following formula was linear regression equation of pNA standard: $Y = 0.0019\ X - 0.002$ ($R^2 = 0.999$, 0–200 μM).

2.15. Measurement of intracellular PKA concentration

The PKA concentration was measured using the PKA ELISA kit, a competitive enzyme immunoassay. Differentiated PC12 cells were plated on 96-well plates at a density of 1×10^4 cells/mL. At the end of treatment, cells were transferred to centrifuge tubes, and the supernatants were collected by centrifugation at $2000 \times g$ for 20 min after repeated freezing and thawing. PKA concentration in the supernatant was measured with an PKA assay kit according to the manufacturer's protocol. The standard curve was fitted to a four-parameter logistic equation according to the following formula: $Y = 0.55232/[1 + (X/0.64678)^{1.00373}] + 0.03823$ ($R^2 = 0.9995$).

2.16. Test for relative expression of BDNF mRNA with Q-PCR

Differentiated PC12 cells were cultured in 6-well plates and treated as described above. Total RNA was isolated using an TaKaRa MiniBEST Universal RNA extraction kit and cDNA was synthesized using PrimeScript RT reagent kit. Quantitative real-time (qRT)-PCR was performed using the ABI 7500 detection system and SYBR Premix Ex Taq II. The primer sequences were listed in Table 1. Briefly, samples were incubated at 95 °C for 30 s following by 40 cycles of 95 °C (5 s), 55 °C (30 s) and 72 °C (30 s). Melting curves were analyzed to ensure that a single amplicon was amplified. The results were analyzed by the $2^{-\triangle\triangle CT}$ method using GAPDH for normalization.

2.17. Western blot analysis of p-CREB

Differentiated PC12 cells (1×10^6 cells/well) were cultured for 24 h and treated as described above. The cellular proteins were extracted with RIPA lysis buffer and protein concentrations were measured using the BCA method (Swets et al., 2018). Equal amounts of protein (30 μg) were subjected to 10% sodium dodecyl sulfate polyacrylamide gel electrophoresis (SDS-PAGE), and transferred to a polyvinylidene fluoride (PVDF) membrane. The membrane was then blocked with 5% BSA for 2 h at room temperature, and subsequently incubated with anti-p-CREB antibodies at 1/1000 final dilution overnight at 4 °C. The membrane was washed three times with TBS-T and incubated with horseradish peroxidase conjugated secondary antibody for 2 h at room temperature. The membrane was washed again followed by incubation with West Pico ECL reagent. The band densities were quantified using an Image J software (National Institutes of Health, USA). All protein quantifications were adjusted for the corresponding GAPDH level.

Table 1
Primer sequences used for amplifying BDNF and GAPDH.

Gene name	Primer sequences
BDNF	Forward 5′-AGCCTCCTCTGCTCTTTCTGCTGGA-3′ Reverse 5′-CTTTTGTCTATGCCCCTGCAGCCTT-3′
GAPDH	Forward 5′-CCAAAAGGGTCATCATCTCC-3′ Reverse 5′-GAGGGGCCATCCACAGTCTT-3′

2.18. Statistical analysis

Data were analyzed with the one-way analysis of variance (ANOVA) followed by Tukey's test GraphPad Prism 5.03 Software (GraphPad Software Inc., San Diego, CA, USA). The results were expressed as the mean ± SEM. Differences between groups were considered to be statistically significant at the $P < 0.05$ level.

3. Results

3.1. Identification of neuroprotective composition in CEE

Phytochemical analysis was performed in order to identify the chemical nature of active principles possibly rendering neuroprotection. Quercetin, caffeine, rutin, L-theanine and ginsenoside Rg1 were found in CEE via ions $[M+H]^+$ at m/z 303.0495, $[M+H]^+$ at m/z 195.0876, $[M+H]^+$ at m/z 611.1613, $[M+H]^+$ at m/z 175.1081, $[M+Na]^+$ at m/z 823.4784, respectively, which were identified by comparison with authentic standards (Fig. 1). Among these compounds, the content of quercetin, rutin and caffeine were 4.60 ± 0.87 mg/g, 3.23 ± 0.83 mg/g, 11.51 ± 0.99 mg/g, respectively, by HPLC analysis.

3.2. Effect of CEE on PC12 cell viability and LDH release under corticosterone treatments

Compared with control group, treatment with 300 μM of corticosterone for 24 h had been shown to cause cytotoxicity in PC12 cells, as evidenced by 62.38 ± 2.69% cell viability loss. Nevertheless, different concentrations of CEE (20, 40, 80 and 160 μg/mL), in the presence of 300 μM corticosterone, significantly increased the cell viability by 79.08 ± 21.17% ($P < 0.05$), 84.90 ± 15.54% ($P < 0.01$), 93.08 ± 11.42% ($P < 0.001$) and 84.43 ± 9.11% ($P < 0.01$), respectively, and revealed significant difference as compared with the corticosterone-treated group (Fig. 2A). The results showed that CEE (20, 40 and 80 μg/mL) could inhibit the corticosterone-induced neurotoxicity with a dose-dependent manner in differentiated PC12 cells.

3.3. Effect of monomer compounds identified in CEE on PC12 cell viability in corticosterone-induced PC12 cells

The safe dose ranges of L-theanine, ginsenoside Rg1, quercetin, rutin and caffeine were screened by investigating toxicity of these compounds in differentiated PC12 cells (Fig. 5S, supplementary material). Furthermore, the neuroprotective effects of five monomer compounds identified in CEE including on corticosterone-treated differentiated PC12 cells were evaluated by using the MTT assay. As shown in Fig. 3, compared with corticosterone-treated group, 400 μM L-theanine, 50 μM ginsenoside Rg1, 5 μM quercetin and 25 μM rutin, in the presence of 300 μM corticosterone, significantly increased the cell viability by 51.35 ± 9.88% ($P < 0.001$), 59.43 ± 7.85. % ($P < 0.001$), 58.89 ± 4.45% ($P < 0.001$) and 57.55 ± 1.48% ($P < 0.005$), respectively. In contrast, 6.25 μM caffeine has a stronger neuroprotective effect and significantly increased the cell viability by 69.69 ± 2.01% ($P < 0.001$) under 300 μM corticosterone co-incubation.

3.4. Effect of CEE on apoptosis in corticosterone-induced PC12 cells by Hoechst 33342 and PI staining

Compared with control cells (Fig. 4A–A), differentiated PC12 cells treated with 300 μM corticosterone for 24 h showed typical characteristics of apoptosis, including condensation of chromatin, the shrinkage of nuclei and plasma membrane changes using Hoechst 33342 staining and PI staining as shown in Fig. 4A and B. By comparison, pretreatment with CEE (20, 40 and 80 μg/mL) in the presence of corticosterone (300 μM), obviously decreased the number of apoptosis cells with a

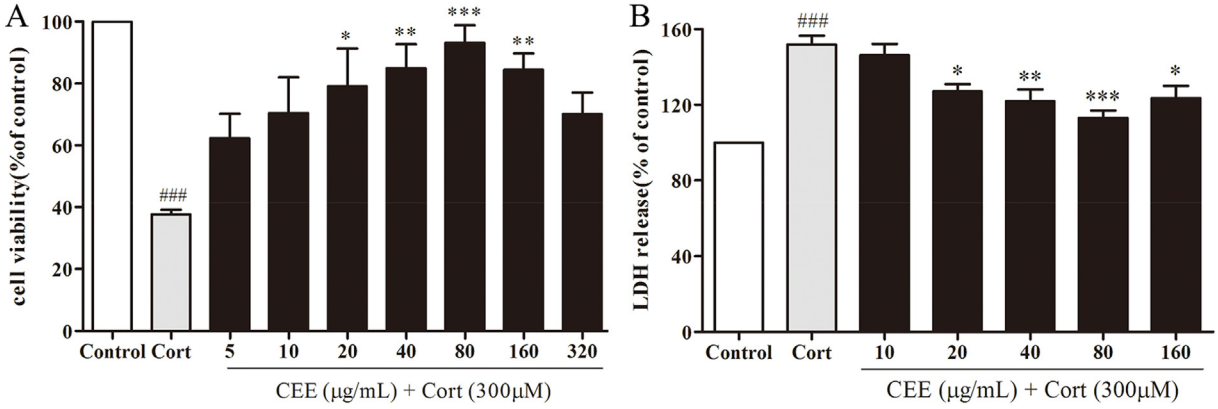

Fig. 2. Effect of CEE on cell viability (A) and LDH release (B) in corticosterone-treated differentiated PC12 cells. Results are presented as means ± SEM (n = 5). $^{###}P < 0.001$ as compared with control group; $^{*}P < 0.05$, $^{**}P < 0.01$ or $^{***}P < 0.001$ as compared with corticosterone-treated group. As shown in Fig. 2B, after treatment with 300 μM corticosterone for 24 h in differentiated PC12 cells, the LDH leakage was obviously increased by 51.90 ± 7.91% ($P < 0.001$) as compared with the control group. However, compared with corticosterone-treated group, different concentrations of CEE (20, 40, 80 and 160 μg/mL) significantly decreased LDH release in cells, and the percentage of LDH leakage were 127.07 ± 6.67% ($P < 0.05$), 121.80 ± 10.79% ($P < 0.01$), 113.00 ± 6.78% ($P < 0.001$) and 123.53 ± 11.05% ($P < 0.05$), respectively.

dose-dependent manner (Fig. 4A[C-E]). Additionally, inhibitory effect of the dose of 160 μg/mL CEE on corticosterone-induced apoptosis was weaker than that of 80 μg/mL (Fig. 4A–F).

3.5. Effect of CEE on internucleosomal DNA fragmentation in corticosterone-induced PC12 cells

A DNA fragmentation assay was used to determine whether the action of CEE was associated with apoptosis or not. A shown in Fig. 4B, DNA isolated from differentiated PC12 cells treated with 300 μM corticosterone showed characteristic DNA ladder formation (lane 2), further corroborating the fact that corticosterone induced apoptosis in differentiated PC12 cells. In addition, DNA from cells co-incubated with 300 μM corticosterone and 20 μg/mL CEE also appeared DNA ladder pattern (lane 3). However, no DNA fragmentation was observed in cells treated with 40, 80 and 160 μg/mL CEE and 300 μM corticosterone co-incubation (lane 4, 5 and 6).

3.6. Effect of CEE on apoptosis rate in corticosterone-induced PC12 cells by AV/PI double staining

As shown in Figs. 4C-1, exposure to corticosterone resulted in the percentage of both early apoptotic cells (AV-FITC$^+$/PI$^-$), late apoptotic cells (AV-FITC$^+$/PI$^+$) and total apoptotic cells increased to 41.40 ± 3.27%, 40.50 ± 3.38%, 81.97 ± 6.74% ($P < 0.05$) as compared to the normal control cells. Cells were co-incubated with 300 μM of corticosterone and different concentrations of CEE for 24 h. After the treatment, the percentage of early apoptotic cells, late apoptotic cells and total apoptotic cells obviously decreased to 32.83 ± 3.84%, 27.90 ± 3.83% and 60.73 ± 7.30% of 20 μg/mL, 26.07 ± 3.26%, 19.13 ± 3.10% and 45.20 ± 6.34% of 40 μg/mL, 14.10 ± 3.94%, 14.47 ± 2.35% and 28.57 ± 6.21% of 80 μg/mL, 29.73 ± 3.10%, 23.30 ± 4.46% and 53.03 ± 7.42% of 160 μg/mL, respectively (Figs. 4C-2). Furthermore, 20, 40 and 80 μg/mL of CEE were used to subsequent studies on neuroprotective molecular mechanism.

3.7. Effect of CEE on corticosterone-induced MMP in PC12 cells

The effect of CEE on corticosterone-induced MMP was assayed by JC-1 staining. JC-1 manifests potential-dependent accumulation, and it accumulates and forms dimeric J-aggregates giving off a bright red fluorescence in the mitochondria in normal cells. However, when the potential is destroyed, the dye cannot access the cytomembrane and remain in the cytoplasm in monomeric form giving off a bright green fluorescence. Therefore, mitochondrial depolarization is expressed by a decrease in the red/green fluorescence intensity ratio. As shown in (Fig. 5A, C), differentiated PC12 cells treated with corticosterone (300 μM) represented a marked decrease in the red/green fluorescence ratio as compared with the control group ($P < 0.05$). In contrast, CEE (20, 40 and 80 μg/mL) pretreatment reduced the effect of corticosterone on the red/green fluorescence intensity ratio (Fig. 5D–F). Consequently, the result showed the restoration of CEE on the MMP in corticosterone-induced differentiated PC12 cells.

3.8. Effect of CEE on corticosterone-induced intracellular Ca^{2+} concentration in PC12 cells

As shown in Fig. 6A, after treatment of differentiated PC12 cells with 300 μM corticosterone for 24 h, the concentration of Ca^{2+} markedly increased to 384.79 ± 19.96 nmol/L as compared with the control group (138.03 ± 20.77 nmol/L) ($P < 0.05$). By contrast, pretreatment with 20, 40 and 80 μg/mL CEE in the presence of 300 μM corticosterone for 24 h observably decreased to 327.74 ± 21.62 nmol/L, 278.93 ± 29.99 nmol/L and 258.76 ± 22.49 nmol/L, respectively.

3.9. Effect of CEE on Bcl-2 and Bax expression ratio in corticosterone-induced PC12 cells

Bcl-2 and Bax proteins are two members of the bcl-2 family that play a prominent role in the regulation of apoptosis, and the ratio of Bcl-2/Bax determined the fate of cell (Xu et al., 2016). Results showed that compared to control cells (1.54), the ratio of Bcl-2 (anti-apoptotic protein) and Bax (pro-apoptotic protein) significantly decreased to 0.31 in cells exposed to 300 μM corticosterone (Fig. 6B). However, pretreatment with 20, 40 and 80 μg/mL CEE increased the ratio of Bcl-2 and Bax to 0.48, 0.89 and 1.03 in corticosterone-treated cells, respectively.

3.10. Effect of CEE on corticosterone-induced ROS in PC12 cells

As shown in Fig. 6C, after exposed to 300 μM corticosterone for 24 h, the intracellular ROS level of differentiated PC12 cells markedly increased by 93.90% relative to the control value (100%, $P < 0.05$), which suggests that corticosterone might induce oxidative stress. When the cells were incubated with different concentrations of CEE (20, 40 and 80 μg/mL) in the presence of 300 μM corticosterone for 24 h, the intracellular ROS levels significantly decreased by 58.54%, 46.95% and

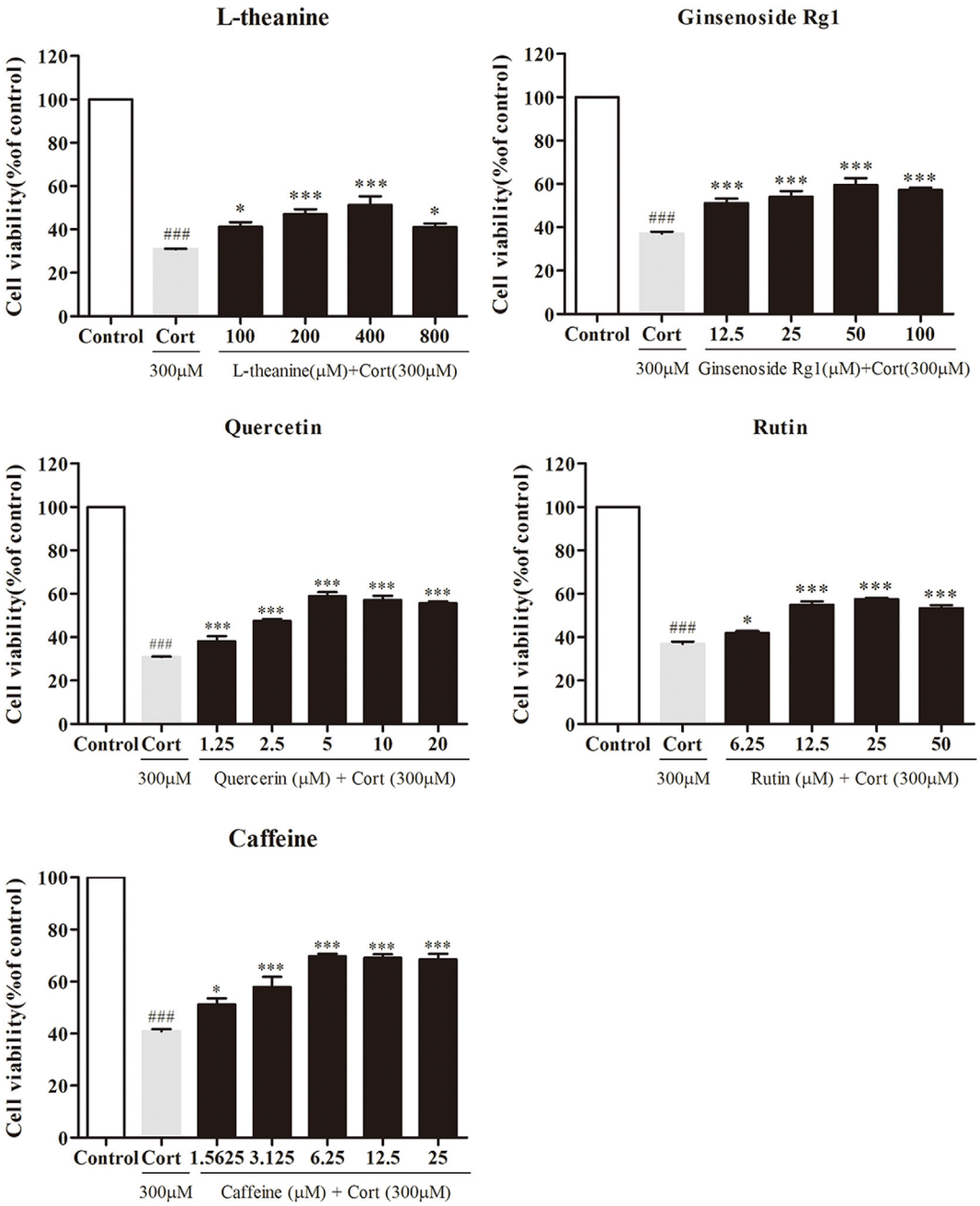

Fig. 3. Effect of each identified components (L-theanine, Ginsenoside Rg1, Quercetin, rutin and Caffeine) in CEE on corticosterone-treated differentiated PC12 cells viability. Results are presented as means ± SEM (n = 5). $^{###}P < 0.001$ as compared with control group; $^{*}P < 0.05$ or $^{***}P < 0.001$ as compared with corticosterone-treated group. Cort: corticosterone.

24.53% ($P < 0.05$) of the control value, respectively.

3.11. Effect of CEE on caspase 9 and caspase-3 levels in corticosterone-induced PC12 cells

To further discuss the underlying mitochondrial apoptotic pathway in the neuroprotective activity of CEE against corticosterone-induced differentiated PC12 cells, the activation of caspase 9 and caspase 3 were also detected. The results showed that the caspase 9 and caspase 3 activities both upregulated in the corticosterone-treated cells compared with the control, whereas CEE (40 and 80 μg/mL) pretreatment caused a significant decrease in caspase 9 and caspase 3 activities (Fig. 6D).

3.12. Effect of CEE on cAMP-dependent protein kinase concentration in corticosterone-induced PC12 cells

We next investigated which signaling pathways are also involved in neuroprotective effect of CEE. PKA/CREB is a important mediator of the signal transduction pathway related to major depression and neural survival (Zeng et al., 2016). We assessed the role of this pathway in the survival promoting effect of CEE in corticosterone-treated differentiated PC12 cells. As shown in Fig. 7A, after treatment of differentiated PC12 cells with 300 μM corticosterone for 24 h, the PKA level markedly decreased to 105.35 ± 8.97 μg/L as compared with the control group (341.04 ± 11.37 μg/L) ($P < 0.05$). By contrast, pretreatment with 20, 40 and 80 μg/mL CEE in the presence of 300 μM corticosterone for 24 h observably increased to 150.35 ± 9.09 μg/L, 168.10 ± 5.68 μg/L and

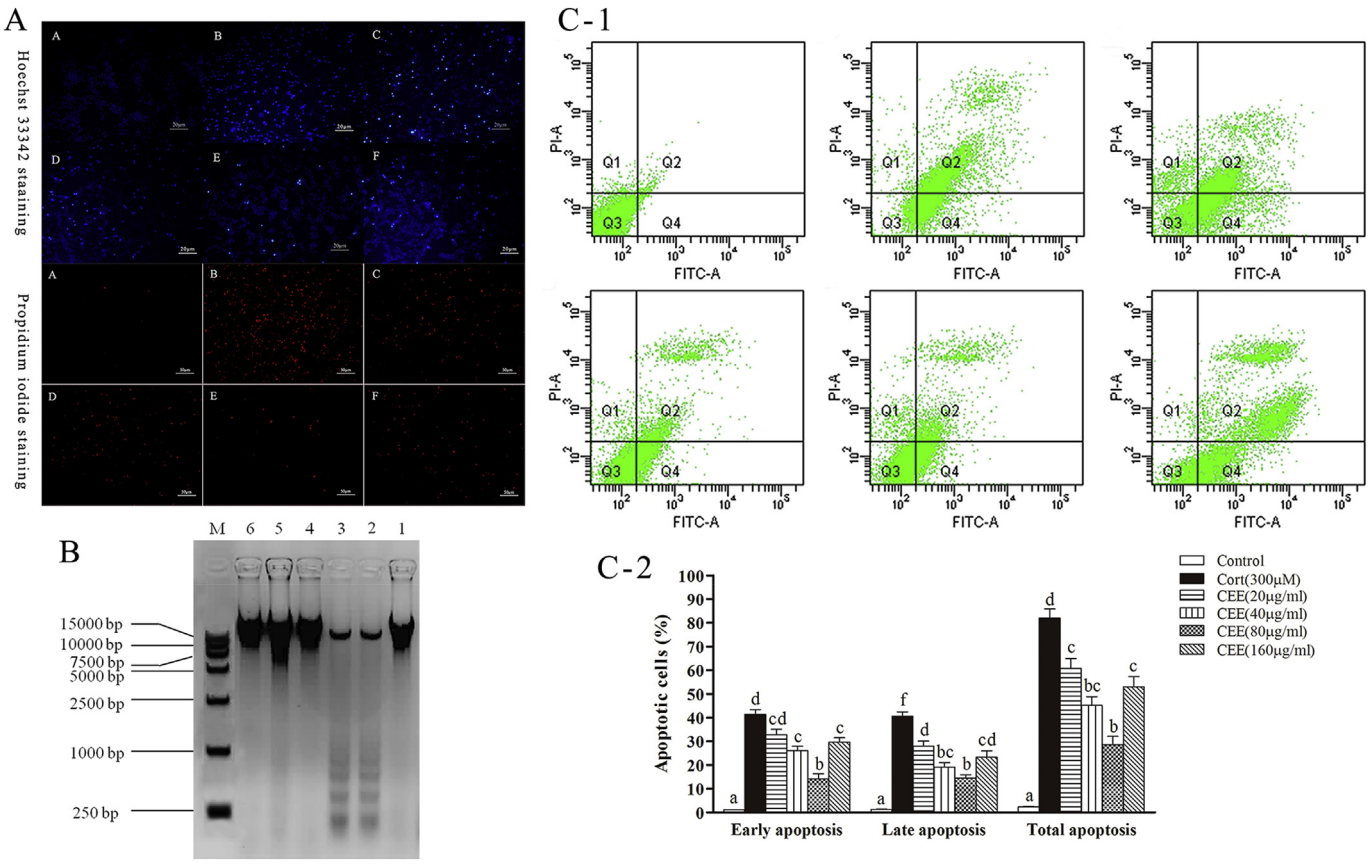

Fig. 4. Effects of CEE on the cell apoptosis in corticosterone-treated PC12 cells by Hoechst 33342 and PI staining, DNA ladder formation, and AV/PI staining. In figure A, A: control; B: 300 μM Cort; C: B + 20 μg CEE; D: B + 40 μg CEE; E: B + 80 μg CEE; F: B + 160 μg CEE; In figure B, M) DNA marker 1) Control cells DNA 2) DNA fragmentation occurrence due to treatment of cells with 300 μM corticosterone 3–6) DNA fragmentation disappearance due to treatment of cells with 20, 40, 80 and 160 μg/ml CEE and 300 μM corticosterone co-incubation; In Figure C-2, Values are presented as mean ± S.E.M (n = 3). Values with different panel letters are significantly different from each other ($P < 0.05$), as determined by Tukey' *t*-test.

198.69 ± 9.74 μg/L, respectively, further supporting the involvement of PKA as a downstream target of CEE.

3.13. Effect of CEE on p-CREB protein expression in corticosterone-induced PC12 cells

As shown in Fig. 7C, compared with the control group, the p-CREB protein expression was obviously down-regulated by 300 μM of corticosterone ($P < 0.05$). However, compared with the corticosterone-treated group, different concentrations of CEE significantly up-regulated the level of p-CREB protein in PC12 cells ($P < 0.05$). The results showed CEE could enhance phosphorylation of CREB via activating PKA.

3.14. Effect of CEE on BDNF mRNA level in corticosterone-induced PC12 cells

Brain-derived neurotrophic factor (BDNF), a CREB downstream target, promotes the survival and growth of neurons during brain development and mediates activity-dependent synaptic plasticity (Yang et al., 2014). The BDNF mRNA expression level in corticosterone-induced differentiated PC12 cells was determined by quantitative real-time (qRT)-PCR. As shown in Fig. 7D, compared with control group, the BDNF mRNA level was obviously down-regulated by 300 μM of corticosterone (1.91 ± 0.28% of control, $P < 0.05$). However, different concentrations of CEE significantly increased the mRNA expression level of BDNF gene compared with corticosterone-treated group (20 μg/mL: 4.16 ± 1.09% of control; 40 μg/mL: 33.51 ± 8.76% of control; 80 μg/mL: 87.62 ± 5.08% of control, $P < 0.05$).

4. Discussion

The PC12 cell line is derived from an induced pheochromocytoma in rats and, when grown in a serum-supplemented medium, PC12 cells exhibit many features of their normal counterparts, adrenal chromaffin cells (Zheng et al., 2012). Additionally, when exposed to nerve growth factor (NGF), PC12 cells acquire a neuronal phenotype similar to that of sympathetic neurons, including the long, branching neurites containing parallel arrays of microtubules, electrical excitability, and egress from the cell cycle. These cells also possess typical features of brain neurons and are richly endowed with glucocorticoid receptors (Adams et al., 2017). In the present study, after treatment of differentiated PC12 cells with 300 μM, cell viability was markedly decreased as evidenced by MTT assay and LDH release assay compared to the untreated control cells, indicating that the cells were physiologically impaired. Importantly, CEE at doses of 20, 40 and 80 μg/mL was able to effectively increase the viability of neurons by protecting them from corticosterone-induced lesion in a dose-dependent manner.

Cell apoptosis, also known as programmed cell death, is characterized by typical morphology including chromatin condensation, formation of apoptotic bodies and controlled degradation of chromosome DNA. Previous studies also have confirmed that the number of apoptotic cells in the hippocampus and cerebral cortex were increased in chronic mild stress model of depressed rats, and could be reduced by antidepressant treatments (Bachis et al., 2008; Liu et al., 2015; Qin et al., 2017). Therefore, apoptosis in hippocampus neurons might be

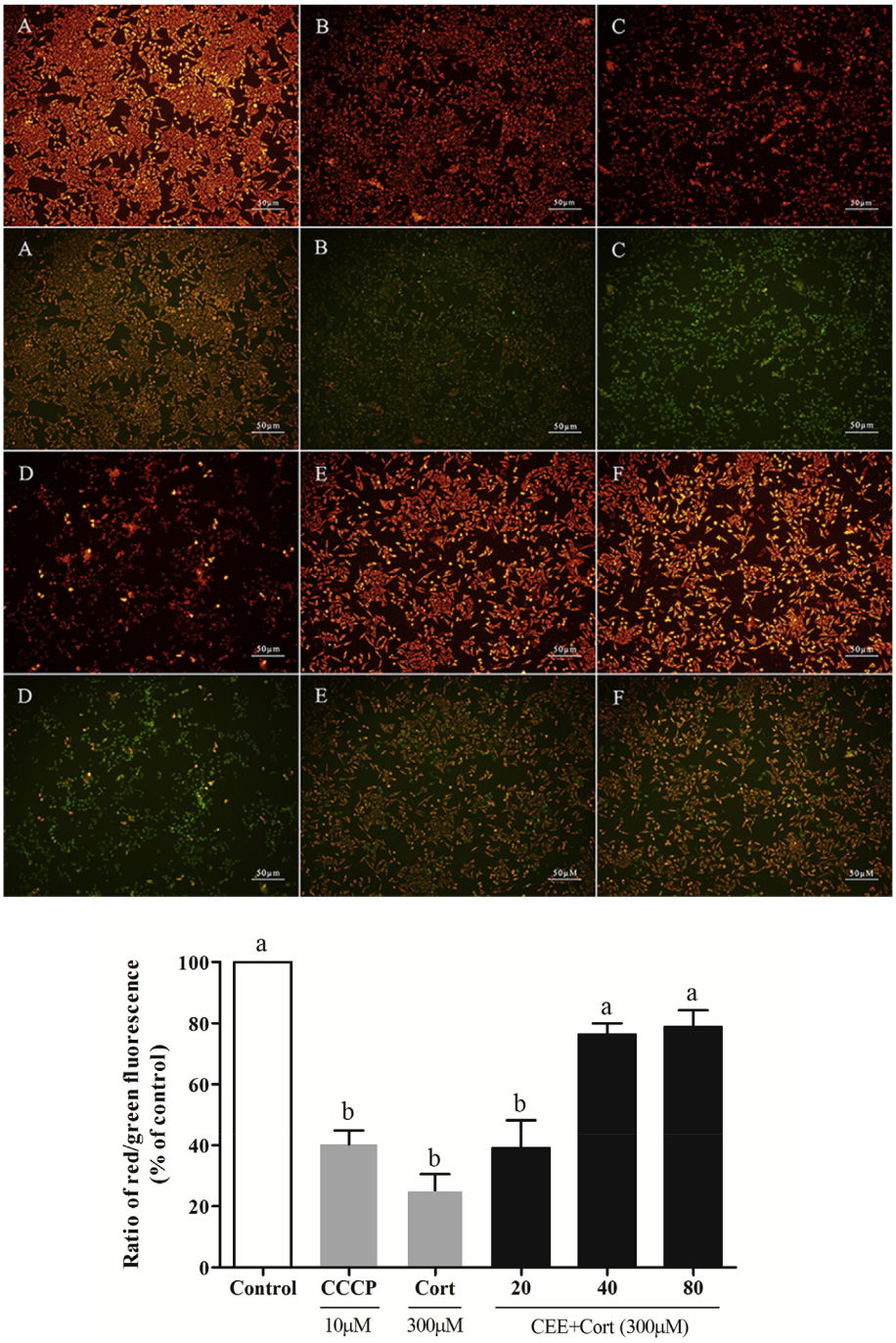

Fig. 5. Effects of CEE on the MMP in corticosterone-treated PC12 cells by JC-1 staining. A: control; B: 10 μm CCCP; C: 300 μM Cort; D: 300 μM Cort + 20 μg CEE; E: 300 μM Cort + 40 μg CEE; F: 300 μM Cort + 80 μg CEE. Values are presented as mean ± S.E.M (n = 3). Values with different panel letters are significantly different from each other ($P < 0.05$), as determined by Tukey' *t*-test.

one of the pathogenetic factors involved in the development of experimental and clinical depression. In this study, CEE suppressed corticosterone-induced early and late apoptosis/necrosis in differentiated PC12 cells compared with the corresponding corticosterone-treated group as evidenced by DNA fragmentation analysis, Hoechst 33342 staining, PI staining and AV-FITC/PI double staining assays, indicating that CEE exerts a neuroprotective effect via inhibiting corticosterone-induced apoptosis of differentiated PC12 cells. Apoptosis in mammals can have one of two initiation phases: the death receptor pathway (extrinsic apoptotic pathways) and the mitochondrial pathway (intrinsic apoptotic pathways), which pathway is selected depends on the nature of the death signal to be integrated (Giorgi et al., 2012). Mitochondria regulates the metabolism and energy balance, as well as control cell apoptosis. Following a apoptotic signal, proapoptotic protein Bax moves from the cytosol to the outer mitochondrial membrane and forms homo-oligomeric complexes, resulting in a hyperpolarization of mitochondrial membrane potential. Subsequently, ROS, cytochrome c and endonuclease G are released from mitochondria into cytoplasm (Estaquier et al., 2012). On the one hand, released ROS is able to destroy the steady state of Ca^{2+} levels within the endoplasmic reticulum (ER), with resulting a intracellular Ca^{2+} overload, and eventually accelerates cells apoptosis (Tabas and Ron, 2011). On the other hand,

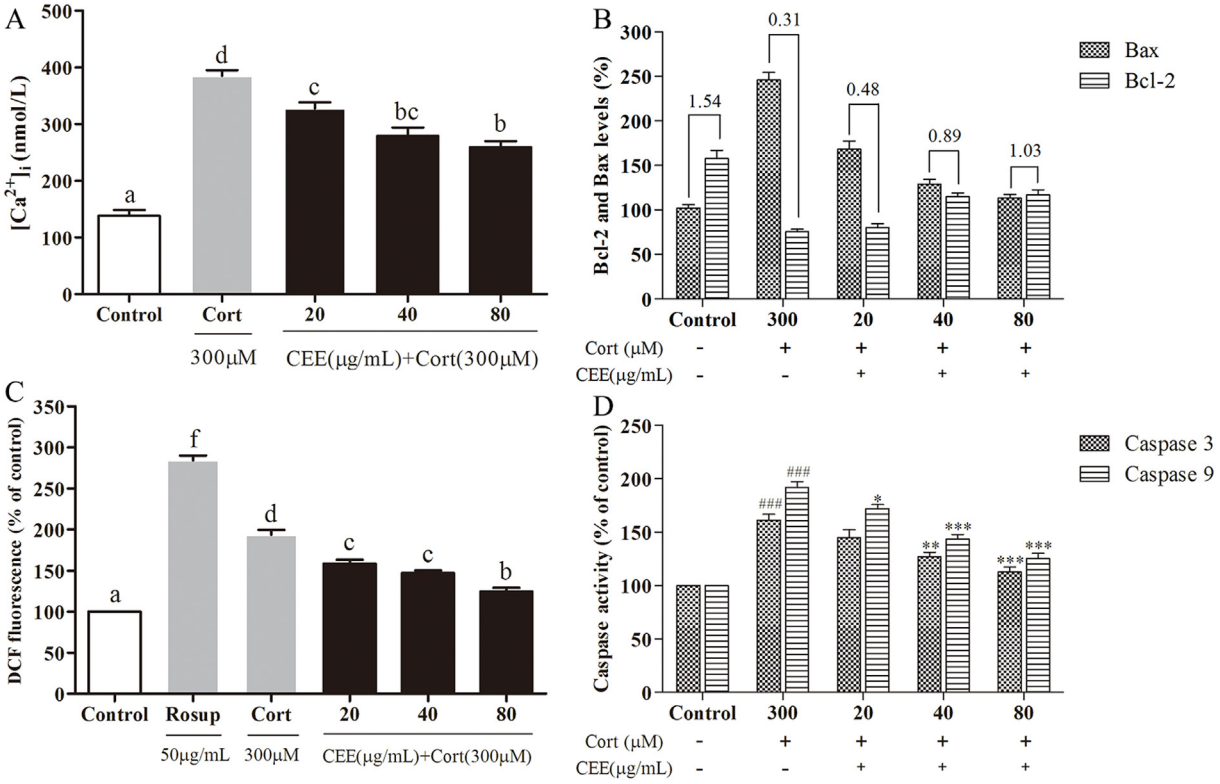

Fig. 6. Effects of CEE on signal molecules in the process of mitochondrial-mediated apoptosis in corticosterone-treated PC12 cell. (A) intracellular Ca^{2+} concentration (B) expression levels of Bcl-2 and Bax (C) intracellular ROS concentration (D) caspase 9 and caspase-3 levels. The digits in figure B represent the ratio of Bcl-2 and Bax levels. Values with different panel letters in figure A and C are significantly different from each other ($P < 0.05$), as determined by Tukey' *t*-test. In figure D, $^{\#\#\#}P < 0.001$ as compared with control group; $^{*}P < 0.05$,$^{**}P < 0.01$ or $^{***}P < 0.001$ as compared with corticosterone-treated group.

cytochrome C released from mitochondria forms apoptosis inducing complex with Apaf-1 and Caspase 9, and then activates Caspase 3, which induces cell apoptosis through specifically cleaving structural proteins (Venkatesh and Suzuki, 2017). Our results have revealed that 20, 40 and 80 μg/mL of CEE not only increased the depolarization of mitochondrial membrane potential and the Bcl-2/Bax expression ratio, but also reduced ROS level, Ca^{2+} concentration and Caspase 3/9 activities, indicating that CEE inhibited corticosterone-induced apoptosis in differentiated PC12 cells by regulating mitochondrial apoptotic pathway.

Pathophysiological studies on depression have recently been gradually transferred to the intracellular secondary messenger system. As an intracellular secondary messenger, cAMP can promote neuronal differentiation and survival as well as outgrowth, regeneration and guidance of neuronal processes, whose signaling has been shown to be implicated in mechanism of reduced synaptic plasticity, that may contribute to the pathphysiology of depression (Wang et al., 2017). cAMP can activate PKA, and subsequently PKA is able to activate CREB by phosphorylation of CREB, thereby further mediating BDNF expression, which plays an important roles in the neuronal survival, maintenance and growth (Xue et al., 2016). Previous studies showed a decreased expression of BDNF in brain regions both in depressive patients and several animal models of depression, suggesting that a decreased BDNF level may be an indicator of vulnerability to develop depression (Bocchio-Chiavetto et al., 2010; Qiao et al., 2017). In this study, the results suggested that CEE could elevate the PKA level, phosphorylation of CREB and mRNA level of BDNF in corticosterone-induced differentiated PC12 cells. It is speculated that the cellular mechanism of CEE against depression involves the PKA-CREB-BDNF signaling pathway.

Phytochemical analysis on CEE revealed the presence of quercetin, rutin, caffeine, L-theanine and ginsenoside Rg1. Quercetin, a flavonoid widely found in plants, has been proved to protect against H_2O_2-induced apoptosis on PC12 cells via activating PI3K/Akt signal pathway (Chen et al., 2016), as well as stimulate NGF-induced neurite outgrowth in PC12 cells via activation of $Na^+/K^+/2Cl^-$ cotransporter (Nakajima et al., 2011). Rutin, a bioflavonoid antioxidant, protects PC12 cells against 6-hydroxydopamine (6-OHDA) induced neurotoxicity through activating superoxide dismutase (SOD), glutathione peroxidase (GPx) and glutathione (GSH) (Magalingam et al., 2013). As an adenosine receptor antagonist, caffeine protects dopaminergic neurons from dopamine-induced neurodegeneration via synergistic adenosine-dopamine D_2-like receptor interactions (Manalo and Medina, 2018). L-theanine as a natural glutamate analog can rapidly distribute through brain stem, hippocampus, cortex and cerebellum, and prevent neuronal apoptosis in hippocampus and cortex after cerebral ischemia (Kim et al., 2009). Ginsenoside Rg1, a well-known three triterpene saponin, protects against oxidative stress-induced neuronal apoptosis through myosin IIA-actin related cytoskeletal reorganization (Wang et al., 2016). Most strikingly, as demonstrated by previous investigators, these compounds mentioned above may be useful agents for the treatment or alleviation of the complex symptoms associated with depressive disorder mediated by different mechanisms (Bahramsoltani et al., 2015). Our data also showed that different concentrations of L-theanine, ginsenoside Rg1, quercetin, rutin and caffeine, in the presence of 300 μM corticosterone, significantly increased the differentiated PC12 cells viability, compared with only corticosterone-treated group. Based on the above studies, we hypothesized that the neuroprotective effect of CEE on corticosterone-induced apoptosis in differentiated PC12 cells depends upon these neuroprotection-related biologically active components mentioned above. Although precise mechanism (s) underlying the neuroprotective effect of CEE and the site of action as well as the biologically active compound (s) responsible for this beneficial property are still not completely clear, it is certain that CEE performs its neuroprotective effect by a multi-target action.

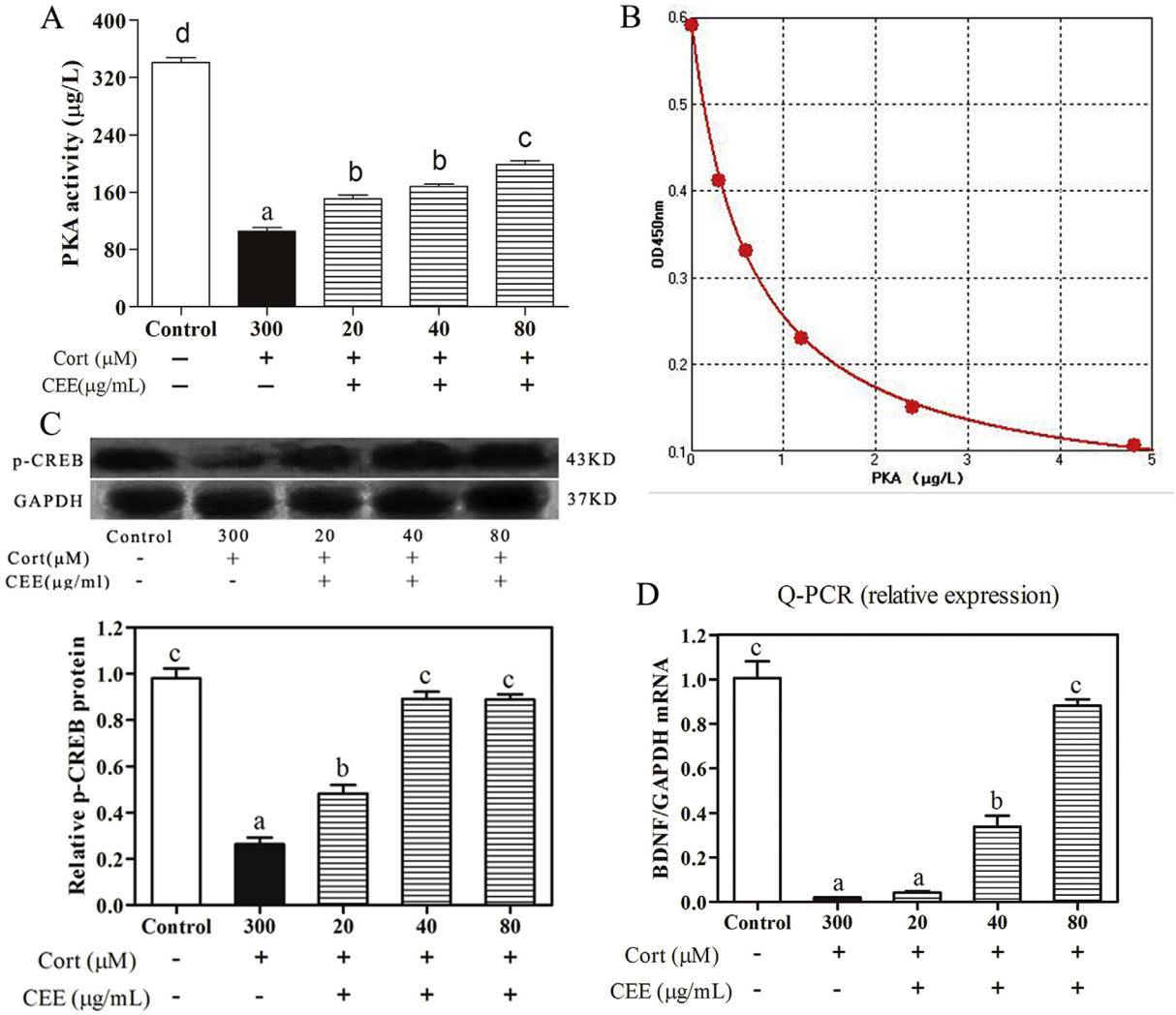

Fig. 7. Effects of CEE on the PKA activity (A), p-CREB protein expression (C) and BDNF mRNA level (D) in corticosterone-induced PC12 cells. The standard curve of PKA in figure B was fitted to a four-parameter logistic equation according to the following formula: $Y = 0.55232/[1 + (X/0.64678)^{1.00373}] + 0.03823 (R^2 = 0.9995)$. Values are presented as mean ± S.E.M (n = 3). Values with different panel letters are significantly different from each other ($P < 0.05$), as determined by Tukey' *t*-test.

5. Conclusions

As far as conclude, our results demonstrated the obviously neuroprotective efficacy of CEE against the impairment induced by corticosterone *in vitro*. This protection is probably associated with inhibition of mitochondria-mediated apoptotic pathway and activation of PKA-CREB-BDNF signal pathway. This neuroprotective effect may be one of the acting mechanisms that accounts for the *in vivo* antidepressant activity of CEE. Overall, these results obtained provides valuable preliminary data on the neuroprotective effect of CEE on corticosterone-induced neuron injury in the pathogenesis of depression that should be useful for the planning of future clinical studies of this plant medicine, thus opening the possibility of its usage as an alternative therapy to depression.

Conflicts of interest

The authors declare that there is no conflict of interests regarding the publication of this paper.

Acknowledgements

This work was supported by the National Public Science and Technology Research Funds Projects of Ocean (201405003) and the Cultivation Plan for Youth Agricultural Science and Technology Innovative Talents of Liaoning Province (2014007). This work was partly supported by the "13th Five-Year" National Key Development Program of China (2016YFD0501406).

Appendix A. Supplementary data

Supplementary data to this article can be found online at https://doi.org/10.1016/j.fct.2019.02.028.

Transparency document

Transparency document related to this article can be found online at https://doi.org/10.1016/j.fct.2019.02.028.

References

Adams, K.W., Kletsov, S., Lamm, R.J., Elman, J.S., Mullenbrock, S., Cooper, G.M., 2017.

Role for Egr1 in the transcriptional program associated with neuronal differentiation of PC12 cells. PLoS One 12 (1), e0170076.
Anderson, D.M., Anderson, K.M., Chang, C.L., Makarewich, C.A., Nelson, B.R., McAnally, J.R., Olson, E.N., 2015. A micropeptide encoded by a putative long noncoding RNA regulates muscle performance. Cell 160 (4), 595–606.
Bachis, A., Cruz, M.I., Nosheny, R.L., Mocchetti, I., 2008. Chronic unpredictable stress promotes neuronal apoptosis in the cerebral cortex. Neurosci. Lett. 442 (2), 104–108.
Bahramsoltani, R., Farzaei, M.H., Farahani, M.S., Rahimi, R., 2015. Phytochemical constituents as future antidepressants: a comprehensive review. Rev. Neurosci. 26 (6), 699–719.
Bocchio-Chiavetto, L., Bagnardi, V., Zanardini, R., Molteni, R., Gabriela Nielsen, M., Placentino, A., Gennarelli, M., 2010. Serum and plasma BDNF levels in major depression: a replication study and meta-analyses. World J. Biol. Psychiatr. 11 (6), 763–773.
Chen, L., Sun, L., Liu, Z., Wang, H., Xu, C., 2016. Protection afforded by quercetin against H2O2-induced apoptosis on PC12 cells via activating PI3K/Akt signal pathway. J. Recept. Signal Transduct. 36 (1), 98–102.
Cowen, P.J., 2010. Not fade away: the HPA axis and depression. Psychol. Med. 40 (1), 1–4.
Estaquier, J., Vallette, F., Vayssiere, J.L., Mignotte, B., 2012. The mitochondrial pathways of apoptosis. Adv. Exp. Med. Biol. 942, 157–183.
Giorgi, C., Baldassari, F., Bononi, A., Bonora, M., De Marchi, E., Marchi, S., Wieckowski, M.R., 2012. Mitochondrial Ca^{2+} and apoptosis. Cell Calcium 52 (1), 36–43.
He, D., Sai, X., Wang, N., Li, X., Wang, L., Xu, Y., 2018a. *Camellia euphlebia* exerts its antidepressant-like effect via modulation of the hypothalamic-pituitary-adrenal axis and brain monoaminergic systems. Metab. Brain Dis. 33 (1), 301–312.
He, D., Wang, X., Zhang, P., Luo, X., Li, X., Wang, L., Xu, Y., 2015. Evaluation of the anxiolytic and antidepressant activities of the aqueous extract from *Camellia euphlebia* Merr. ex Sealy in mice. Evid-Based. Compl. Alt., 618409.
He, D., Zhang, P., Sai, X., Li, X., Wang, L., Xu, Y., 2018b. *Camellia euphlebia* flower extract inhibits oleic acid-induced lipid accumulation via reduction of lipogenesis in HepG2 cells. Eur. J. Integr. Med. 17, 1–8.
Huang, Y., Coupland, N.J., Lebel, R.M., Carter, R., Seres, P., Wilman, A.H., Malykhin, N.V., 2013. Structural changes in hippocampal subfields in major depressive disorder: a high-field magnetic resonance imaging study. Biol. Psychiat. 74 (1), 62–68.
Huang, Y.L., Qiu, R.F., Mai, W.Y., Kuang, J., Cai, X.Y., Dong, Y.G., Jiang, Z.G., 2012. Effects of insulin-like growth factor-1 on the properties of mesenchymal stem cells in vitro. J. Zhejiang Univ. - Sci. B 13 (1), 20–28.
Jiang, Y., Li, Z., Liu, Y., Liu, X., Chang, Q., Liao, Y., Pan, R., 2015. Neuroprotective effect of water extract of Panax ginseng on corticosterone-induced apoptosis in PC12 cells and its underlying molecule mechanisms. J. Ethnopharmacol. 159, 102–112.
Keller, J., Gomez, R., Williams, G., Lembke, A., Lazzeroni, L., Murphy Jr., G.M., Schatzberg, A.F., 2017. HPA axis in major depression: cortisol, clinical symptomatology and genetic variation predict cognition. Mol. Psychiatr. 22 (4), 527.
Kim, T.I., Lee, Y.K., Park, S.G., Choi, I.S., Ban, J.O., Park, H.K., Hong, J.T., 2009. L-Theanine, an amino acid in green tea, attenuates β-amyloid-induced cognitive dysfunction and neurotoxicity: reduction in oxidative damage and inactivation of ERK/p38 kinase and NF-κB pathways. Free Radical Biol. Med. 47 (11), 1601–1610.
Liu, B., Xu, C., Wu, X., Liu, F., Du, Y., Sun, J., Dong, J., 2015. Icariin exerts an antidepressant effect in an unpredictable chronic mild stress model of depression in rats and is associated with the regulation of hippocampal neuroinflammation. Neuroscience 294, 193–205.
Magalingam, K.B., Radhakrishnan, A., Haleagrahara, N., 2013. Rutin, a bioflavonoid antioxidant protects rat pheochromocytoma (PC-12) cells against 6-hydroxydopamine (6-OHDA)-induced neurotoxicity. Int. J. Mol. Med. 32 (1), 235–240.
Manalo, R.V., Medina, P., 2018. Caffeine protects dopaminergic neurons from dopamine-induced neurodegeneration via synergistic adenosine-dopamine D_2-like receptor interactions in transgenic Caenorhabditis elegans. Front. Neurosci. 12, 137.
Micale, V., Drago, F., 2018. Endocannabinoid system, stress and HPA axis. Eur. J. Pharmacol. 834, 230–239.
Miller, B.R., Hen, R., 2015. The current state of the neurogenic theory of depression and anxiety. Curr. Opin. Neurobiol. 30, 51–58.
Morabito, C., Guarnieri, S., Fanò, G., Mariggiò, M.A., 2010. Effects of acute and chronic low frequency electromagnetic field exposure on PC12 cells during neuronal differentiation. Cell. Physiol. Biochem. 26 (6), 947–958.
Nakajima, K.I., Niisato, N., Marunaka, Y., 2011. Quercetin stimulates NGF-induced neurite outgrowth in PC12 cells via activation of $Na^+/K^+/2Cl^-$ cotransporter. Cell. Physiol. Biochem. 28 (1), 147–156.
Pariante, C.M., Lightman, S.L., 2008. The HPA axis in major depression: classical theories and new developments. Trends Neurosci. 31 (9), 464–468.
Qiao, H., An, S.C., Xu, C., Ma, X.M., 2017. Role of proBDNF and BDNF in dendritic spine plasticity and depressive-like behaviors induced by an animal model of depression. Brain Res. 1663, 29–37.
Qin, T., Fang, F., Song, M., Li, R., Ma, Z., Ma, S., 2017. Umbelliferone reverses depression-like behavior in chronic unpredictable mild stress-induced rats by attenuating neuronal apoptosis via regulating ROCK/Akt pathway. Behav. Brain Res. 317, 147–156.
Smith, K., 2014. Mental health: a world of depression. Nature 515 (7526), 180–181.
Swets, M., Wouters, A., Krijgsman, D., van Vlierberghe, R.L., Boot, A., van Eendenburg, J.D., Kuppen, P.J., 2018. HLA-G protein expression in colorectal cancer evaluated by immunohistochemistry and western blot analysis: its expression characteristics remain enigmatic. Clin. Immunol. 194, 80–86.
Tabas, I., Ron, D., 2011. Integrating the mechanisms of apoptosis induced by endoplasmic reticulum stress. Nat. Cell Biol. 13 (3), 184–190.
Venkatesh, S., Suzuki, C.K., 2017. HSP60 Takes a hit: inhibition of mitochondrial protein folding. Cell Chem. Biol. 24 (5), 543–545.
Vos, T., Allen, C., Arora, M., Barber, R.M., Bhutta, Z.A., Brown, A., et al., 2016. Global, regional, and national incidence, prevalence, and years lived with disability for 310 diseases and injuries, 1990–2015: a systematic analysis for the Global Burden of Disease Study 2015. The Lancet 388 (10053), 1545–1602.
Wang, C., Guo, J., Guo, R., 2017. Effect of XingPiJieYu decoction on spatial learning and memory and cAMP-PKA-CREB-BDNF pathway in rat model of depression through chronic unpredictable stress. BMC Complement Altern. Med. 17 (1), 73.
Wang, Y., Liu, Q., Xu, Y., Zhang, Y., Lv, Y., Tan, Y., Cao, Z., 2016. Ginsenoside Rg1 protects against oxidative stress-induced neuronal apoptosis through myosin IIA-actin related cytoskeletal reorganization. Int. J. Biol. Sci. 12 (11), 1341–1356.
World Health Organization, 2017. Depression and Other Common Mental Disorders: Global Health Estimates. pp. 1–24.
Wu, F., Li, H., Zhao, L., Li, X., You, J., Jiang, Q., Xu, Y., 2013. Protective effects of aqueous extract from *Acanthopanax senticosus* against corticosterone-induced neurotoxicity in PC12 cells. J. Ethnopharmacol. 148 (3), 861–868.
Xu, G., Kuang, G., Jiang, W., Jiang, R., Jiang, D., 2016. Polydatin promotes apoptosis through upregulation the ratio of Bax/Bcl-2 and inhibits proliferation by attenuating the β-catenin signaling in human osteosarcoma cells. Am. J. Transl. Res. 8 (2), 922–931.
Xue, W., Wang, W., Gong, T., Zhang, H., Tao, W., Xue, L., Chen, G., 2016. PKA-CREB-BDNF signaling regulated long lasting antidepressant activities of Yueju but not ketamine. Sci. Rep. 6, 26331.
Yang, J.L., Lin, Y.T., Chuang, P.C., Bohr, V.A., Mattson, M.P., 2014. BDNF and exercise enhance neuronal DNA repair by stimulating CREB-mediated production of apurinic/apyrimidinic endonuclease 1. Neuromol. Med. 16 (1), 161–174.
Zeng, B., Li, Y., Niu, B., Wang, X., Cheng, Y., Zhou, Z., Xu, J., 2016. Involvement of PI3K/Akt/FoxO3a and PKA/CREB signaling pathways in the protective effect of fluoxetine against corticosterone-induced cytotoxicity in PC12 cells. J. Mol. Neurosci. 59 (4), 567–578.
Zhao, Z., Liu, X., Shi, S., Li, H., Gao, F., Zhong, X., Wang, Y., 2018. Exogenous hydrogen sulfide protects from endothelial cell damage, platelet activation, and neutrophils extracellular traps formation in hyperhomocysteinemia rats. Exp. Cell Res. 370 (2), 434–443.
Zheng, M., Liu, C., Pan, F., Shi, D., Zhang, Y., 2012. Antidepressant-like effect of hyperoside isolated from *Apocynum venetum* leaves: possible cellular mechanisms. Phytomedicine 19 (2), 145–149.
Zou, Y., Wang, B., Fu, W., Zhou, S., Nie, Y., Tian, S., 2016. Apelin-13 protects PC12 cells from corticosterone-induced apoptosis through PI3K and ERKs activation. Neurochem. Res. 41 (7), 1635–1644.